Reprinted from ENVIRONMENTAL SCIENCE & TECHNOLOGY, Vol. 26, 1992

Laser Microprobe Mass Analysis of Individual North Sea Aerosol Particles

I. Dierck, D. Michaud,† L. Wouters, and R. Van Grieken*

Department of Chemistry, University of Antwerp (U.I.A.), Universiteitsplein 1, B-2610 Antwerp-Wilrijk, Belgium

■ Some 6000 individual aerosol particles in the 0.5–4-μm aerodynamic diameter range, collected from an aircraft at different heights above the North Sea, were analyzed using laser microprobe mass analysis (LAMMA). In this way, various well-separated particle types could be defined. Many of these particles appeared to occur as internal mixtures. Several definite trends in particle type abundances as a function of wind direction during sampling and of particle size could be observed. This helped in identifying source processes of the aerosol. Obtaining conclusive results as a function of sampling height, on the other hand, was much less straightforward. This is not surprising, since most samples were collected under the inversion layer where extensive mixing is likely to take place.

Introduction

Considerable attention has already been paid to the determination of atmospheric particles from various regions all over the world. These observations aim to establish a global balance of man's pollutants into the air as compared to natural input.

The aerosols discussed in this paper were sampled over the Southern Bight of the North Sea, an area closely surrounded by anthropogenic pollution sources. The present work is part of a study concerning the atmospheric deposition of heavy metals into the North Sea, involving bulk as well as single-particle analyses. Individual particle analysis was performed by electron probe X-ray microanalysis (EPXMA), the results of which are presented elsewhere (*1*), and by laser microprobe mass analysis (LAMMA). EPXMA gives quantitative results about the major chemical composition of a particle, but fails to detect elements with $Z < 11$; hence, for example, ammonium compounds, which are very important from an environmental point of view, will go unnoticed. LAMMA can fill this gap. Furthermore, it can provide information about trace elements (its detection limits, although element-dependent, are generally a factor of 10 or more better than those of EPXMA) and possibly about surface coatings and organic components. Cluster ion formation in the laser plasma and different sensitivities might however obscure the compositional information to some extent. LAMMA is less automated than EPXMA, hence much more labor intensive and less appropriate to analyze huge amounts of particles.

Experimental Section

Analytical Technique. In the LAMMA-500 instrument (Leybold-Heraeus, Cologne, Germany), individual aerosol particles are vaporized by a single high-power laser pulse (τ = 15 ns) of a Q-switched frequency-quadrupled Nd:YAG laser (λ = 265 nm; power density 10^7–10^{11} W·cm^{-2}). The resulting microplasma contains atomic and molecular ions, as well as electrically neutral fragments. Depending on the spectrum polarity chosen, positive or negative ions are accelerated and collimated into the drift tube of a time-of-flight mass spectrometer, where they are separated according to their m/z ratios. The signal is then fed into a 32-KB memory transient recorder (LeCroy TR8818) and digitized. Spectra are stored on a personal computer for off-line data handling. Groups of spectra can be automatically calibrated, integrated, and compared to a library of standard spectra, which can be complemented by the user (*2*). All software applied is homemade. The instrument and part of the software package are discussed extensively by Verbueken et al. (*3*) and Van Espen et al. (*4*).

Sampling Procedure. Aerosol samples were collected under predominantly cloudless conditions during six different flights with a twin engine aircraft Piper Chieftain (PA 31-350 PH-ECO) of Geosens B.V. Company (Rotterdam, The Netherlands). At the beginning of each flight, an upward spiral was flown at the Goeree Platform (51°-55.5′N, 3°40.0′E), while SO_2 and O_3 concentrations, temperature, and dew point were continuously monitored to localize the inversion height. From there, for each flight, six tracks of 120 km were flown over the North Sea in the direction of the wind; the six tracks were about equally spaced between the sea surface and the boundary layer. For every track, a sample for LAMMA was obtained by means of five-stage single-orifice Batelle-type impactors,

† On leave from the Department of Physics, Laval University, Québec, Canada.

 0013-936X/92/0926-0802$03.00/0

Table I. General Flight Data

flight	flight date	wind sector	source area[a]	inversion height, m	wind speed at ground level, $m \cdot s^{-1}$
1	01/13/89	S + W	marine, F	1750	13.6
2	01/23/89	S + W	marine, F	950	10.8
3	03/06/89	S	NL, B, F	400	9.5
4	03/12/89	diverse	marine, UK, NL, B	800	8.8
5	05/23/89	E	NL, G, CS, PL	1500	7.8
6	05/23/89	E	G, CS, PL	1500	8.9

[a] Abbreviations are as follows: F, France; NL, The Netherlands; B, Belgium; UK, United Kingdom; G, Germany; CS, Czechoslovakia; PL, Poland.

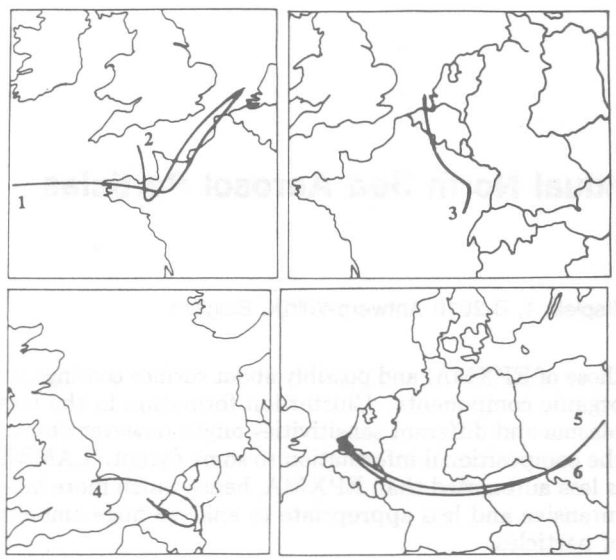

Figure 1. Back-trajectories for the flights 1–6.

equipped with Formvar (i.e., a slightly adhesive polymer) coated electron microscope grids and operated at a flow rate of 1 $L \cdot min^{-1}$. The 50% cutoff aerodynamic diameters of stages 1–5 are 4, 2, 1, 0.5, and 0.25 μm, respectively. A sampling time of ca. 25 min usually provided a satisfactory loading for LAMMA. In order to avoid distortion of the particle size distribution, sampling was performed under isokinetic conditions. In this case, the Pennsylvania State University (PSU) isokinetic sampler designed by Pena et al. (*5*) was used. The sampler was mounted on the roof of the aircraft in such a way that the intake was located outside the boundary layer of the aircraft and that no particulate or gaseous matter coming from the exhaust of the engines could be sampled. Until analysis, the samples were stored in sealed PVC Petri dishes. For each flight, four 36-h "backward in time air trajectories" (or "back-trajectories" for short) were calculated for four different levels (1000, 900, 850, and 700 mbar), providing valuable information about the source regions of the air masses. They were interpolated to yield trajectories for the six different flight levels (*1*). Figure 1 shows the back-trajectories for the different flights at 1000 mbar (sea level). General flight data (flight date, wind sector, prevailing source areas as determined from the back-trajectories, inversion height, and wind speed at ground level) are listed in Table I.

A total of some 120 samples were investigated, namely five impactor stages for four to six tracks of six flights. For each of these impactor stages, some 50 particles were randomly selected for LAMMA, resulting in approximately 6000 positive-mode spectra. With LAMMA being a destructive technique, it is impossible to record a positive-mode and a negative-mode spectrum of one particle without introducing uncertainties concerning preferential evaporation and focusing errors. The major part of this work was performed on positive-mode spectra, because they are advantageous for the identification of trace metals. Negative-mode spectra were used in an attempt to extract additional information concerning the determination of certain anions.

Results and Discussion

EPXMA of some 25 000 similar aerosol particles, sampled in a time span of 4 years from a research vessel over the North Sea, led to the definition of some well-separated particle types: sea salt, aluminosilicates, S-rich, Ca- and S-rich, Ca-rich, Si-rich, Ti-rich, and Fe-rich (*6*). Preliminary investigation of a representative sample of LAMMA spectra revealed the presence of all these particle types, but a great part of them appeared to occur as internal mixtures. For the particles of stage 5 (aerodynamic cutoff diameter of 0.25 μm) this might be an artifact, because part of them are beyond observation by the optical microscope the LAMMA is equipped with; in other words, one never knows if only one particle has been ablated by a laser shot. On the other stages, however, particles are generally well separated on the grids, so in this case, "mixed spectra" unambiguously point to internally mixed particles. These mixtures were already discussed by Andreae et al. (*7*), who attributed them to processes within clouds.

All spectra were automatically screened for the presence of compounds that characterize the different groups and their particular features. Special attention was paid to the occurrence of trace metals not detectable by EPXMA. As the limited mass resolution of the LAMMA does not allow it to distinguish different ions of the same nominal mass, the problem of possible misclassification was carefully evaluated. Generally, the possibility for misclassification diminishes when the number of peaks necessary for a positive evaluation increases. This possibility however also depends on the spectral region. A peak at $m/z = 18$ (NH_4^+) can, at least for this kind of sample, without further consideration be attributed to an ammonium compound. On the other hand, it is our experience that the identification of Cu suffers seriously from spectral interferences, even when isotopic abundances are used for peak recognition. Therefore, it was decided to omit Cu from the set of investigated metals. For the same reason, Ni and Mn were left out. As, ordinarily, metal ions always appear together with at least one metal oxide ion, these oxides were also included in the sets of peaks necessary for the identification of the elements which occur in the most crowded region of the spectrum (i.e., from $m/z = 39$ to $m/z = 165$).

In this work, the results obtained by LAMMA are discussed as a function of wind direction during sampling, of particle size and of sampling height. When the corresponding figures are being interpreted, it should be kept in mind that LAMMA has different sensitivities for different compounds; the sensitivity for Na^+ is some 150 times

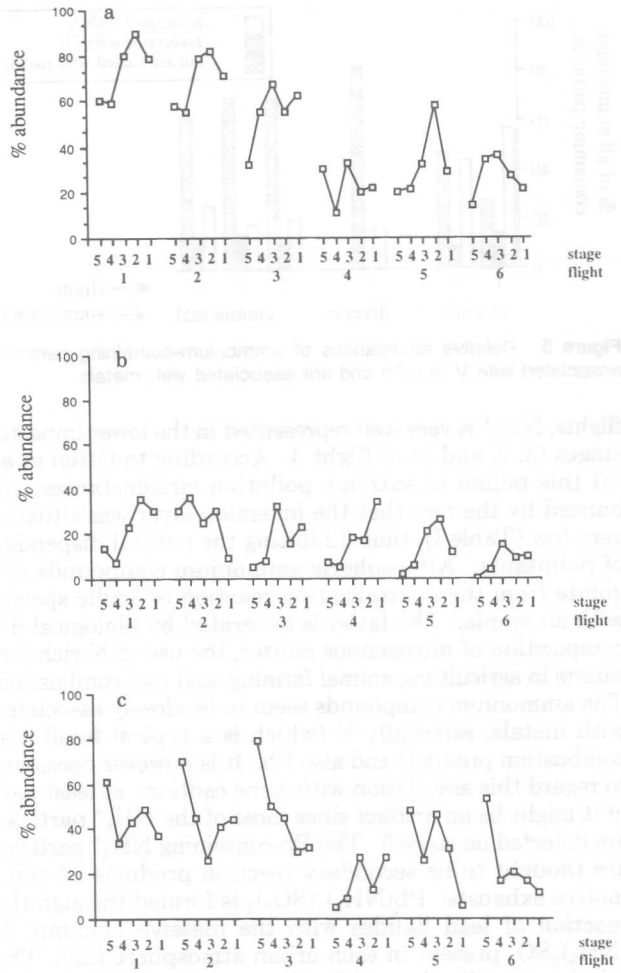

Figure 2. Relative abundances of (a) sea salt, (b) $NaNO_3$-containing, and (c) Na_2SO_4-containing particles, averaged per stage over all impactors for each flight.

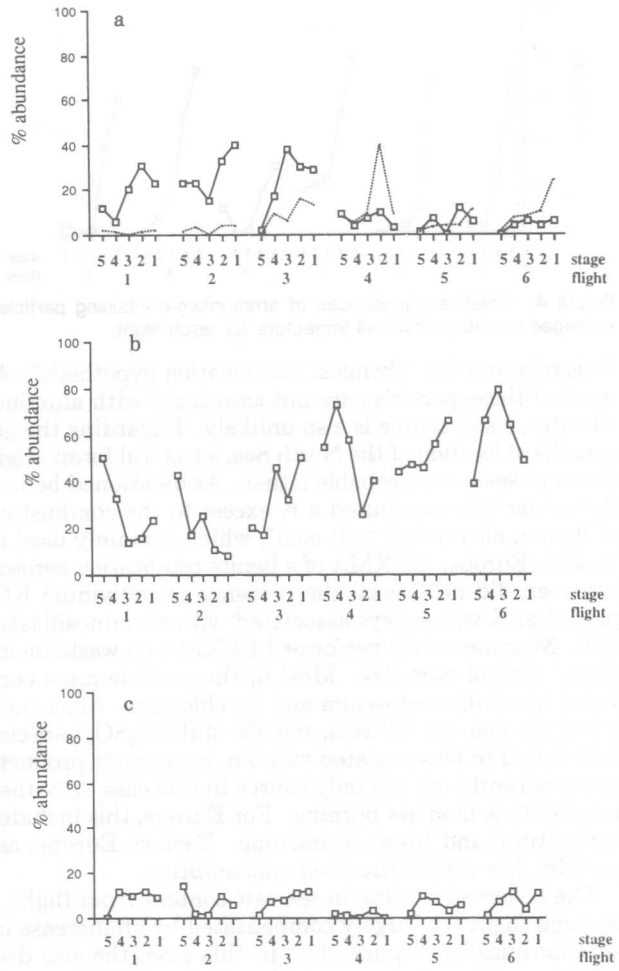

Figure 3. Relative abundances of (a) KCl-containing particles, (b) aluminosilicates, and (c) Ca-rich particles, averaged per stage over all impactors for each flight.

better than that for NH_4^+ (*8*). Differences in overall peak intensities between *different* compounds are thus by no means indicative for concentration differences.

Standard seawater spectra are largely dominated by the typical Na_xCl_y cluster ions (*9*). Therefore, a particle is considered a sea salt particle or a mixed particle containing sea salt when NaCl is detected by the search routine. Figure 2a shows the relative abundances of sea salt particles (i.e., the percentage of particles containing sea salt), averaged per stage over all impactors for each flight. The size profiles are fairly consistent over all flights. The highest abundances are reached among the particles of stage 2 or stage 3. Comparing different flights, the total sea salt content is highest for flights 1 and 2. This can be explained by two factors: longer time spent over the sea by the sampled air masses and highest wind speed during sampling for the first two flights; and an increased wind speed promoting sea salt particle production (*10*).

Sea salt can be transformed in the atmosphere by heterogeneous reactions with H_2SO_4 and/or HNO_3 vapor (*11*). These alterations are reflected in the spectra by the appearance of peaks indicative for $NaNO_3$ and Na_2SO_4 (i.e., the normal Na/O clusters and $Na_2NO_2^+$, $Na_2NO_3^+$ and $Na_3SO_3^+$, $Na_3SO_4^+$, respectively). Their size profiles are reported in Figure 2, panels b and c. Sometimes, the transformation is so complete that the Na_xCl_y clusters are not detectable any more. In this case, the particle is no longer considered a sea salt particle. Most of the $NaNO_3$ profiles match those of NaCl rather closely; this is not surprising inasmuch as 81% of all detected $NaNO_3$ was found to be associated with NaCl. The Na_2SO_4 abundance patterns, on the other hand, are very different. Except for flight 4, they are all characterized by a maximum abundance in the smallest size ranges. The NaCl to Na_2SO_4 conversion rate increases as the particle diameter decreases; as a consequence, the small particles have a high Cl^- deficiency and SO_4^{2-} enrichment, so Cl^- is very often not detectable in their spectra any more. $NaNO_3$ is not as abundant in the small-particle fraction as Na_2SO_4. This corresponds with the findings of Savoie and Prospero (*12*) and Mallant et al. (*11*), who state that the fact that HNO_3 has a much higher vapor pressure than H_2SO_4 leads to the removal of HNO_3 when condensing H_2SO_4 lowers the surface pH of the small particles.

KCl is a minor sea salt component. In standard seawater aerosols, K_xCl_y clusters appear when the Na_xCl_y clusters are in overflow. Some 35% of the KCl particles, however, do not exhibit the typical Na_xCl_y mass peaks in their spectra. These particles sometimes seem to have undergone the same transformations as sea salt: K_2SO_4 and KNO_3 peaks are regularly detected. K enrichments relative to Na have already been observed in marine aerosols. These excesses have been attributed to chemical fractionation at the air–sea interface (*13*), to soil sources (*14*), biomass combustion (*15*), waste incinerator products (*16*), long-range tropical forest aerosol transport (*17*), and the combustion of lignite (*18*). Figure 3a shows the abundance patterns of KCl particles with and without NaCl association. The relative concentrations of the latter are higher when the sampled air masses have a nonmarine origin.

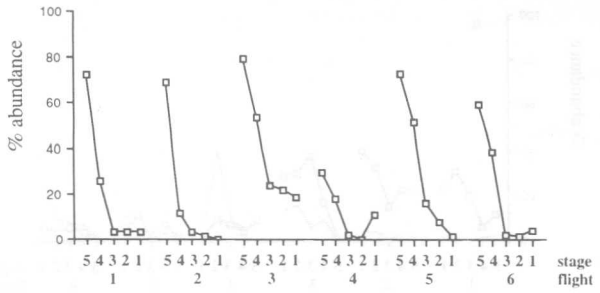

Figure 4. Relative abundances of ammonium-containing particles, averaged per stage over all impactors for each flight.

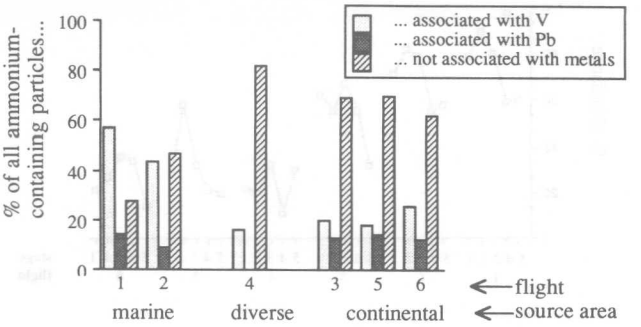

Figure 5. Relative abundances of ammonium-containing particles, associated with V and Pb and not associated with metals.

This rules out the "chemical fractionation hypothesis". As most of these particles are not associated with aluminosilicates, a soil source is also unlikely. Regarding the geographical location of the North Sea, a tropical forest origin does not seem too probable either. As mentioned before, Schneider (*18*) attributed a K excess to the combustion of lignite, also called "salt coal", which is mainly used in Eastern Europe. EPXMA of a lignite combustion aerosol, however, did not reveal the presence of individual KCl particles; K was always associated with aluminosilicates (*19*). Mammane (*16*) performed EPXMA on waste incinerator aerosol particles. Most of the particle mass consisted of soluble potassium and Zn chlorides. Since only 3% of the non–sea salt KCl, and 5% of the K_2SO_4 particles were found to be associated with Zn, incinerator products are apparently not the only source in this case. Another possibility is biomass burning. For Europe, this includes agricultural and firewood burning. Eastern Europe, especially, has a high firewood consumption.

The observed decline in sea salt content from flight 1 through flight 6 is largely compensated by an increase in aluminosilicates (Figure 3b). In this case, the size distribution pattern is very variable, which might be caused by the fact that two sources are responsible for this particle type: soil dust and fly ash. According to our experience, they are indistinguishable on the basis of their LAMMA spectra. Only those fly ash particles formed at high combustion temperatures can be identified because of their globular appearance.

For identification purposes, Ca-rich particles are defined as particles whose spectra display the typical $(CaO)_x$ and $(CaO)_xCa$ cluster ions. Analyses of Ca standards show that all Ca- and O-containing compounds provide those ions in their LAMMA spectra. According to the literature, the most plausible sources for Ca-rich particles are fractional crystallization and subsequent breaking of sea salt droplets (*7*), marine biogenic material (*7*), calcite contained in soil dust (*20*), and combustion processes (*21*). In an earlier, very extensive EPXMA investigation of North Sea aerosol particles, Ca-rich and Ca- and S-rich particles were detected (*6*). The Ca- and S-rich particles were clearly continential-derived while the Ca-rich could not be unambiguously assigned to one source type. With LAMMA, however, $CaCO_3$ and $CaSO_4$ are indistinguishable on the basis of their positive-mode spectra. $Ca_3(PO_4)_2$, on the other hand, displays some typical $CaPO_x$ peaks. Figure 3C shows the Ca-rich particle type size distributions averaged over all impactors per flight. In this case, no clear differences can be derived between marine and continental air masses.

Figure 4 shows the percent abundance of NH_4^+-containing particles, averaged per stage over all impactors for each flight. NH_4^+ seems to be mainly present in the smallest particles. Its size distribution pattern is consistent through all flights. The total relative NH_4^+ concentration for flight 4 is definitely the lowest. Compared to all other flights, NH_4^+ is very well represented in the lower impactor stages (3, 2, and 1) of flight 3. According to Otten et al. (*8*) this points to extreme pollution circumstances, enhanced by the fact that the inversion layer was situated very low (Table I), thus inhibiting the natural dispersion of pollutants. Atmospheric ammonium compounds originate from the neutralization reaction of acidic species with ammonia. The latter is generated by biological decomposition of nitrogenous matter, the use of N-rich fertilizers in agriculture, animal farming, and coal combustion. The ammonium compounds seem to be closely associated with metals, especially V (which is a typical fossil fuel combustion product) and also Pb. It is however necessary to regard this association with some caution: at least part of it might be an artifact since most of the NH_4^+ particles are detected on stage 5. The Pb-containing NH_4^+ particles are thought to be secondary reaction products of automotive exhausts: $Pb(NH_4)_2(SO_4)_2$ is formed through the reaction of lead halides with the massive amounts of $(NH_4)_2SO_4$ present in each urban atmosphere (*22*). The relative contribution of the V-containing NH_4 particles decreases when the sampled air masses have passed over Europe (Figure 5). This could be explained by an ammonia input from agricultural activities in The Netherlands and the northwestern part of Belgium. The relative amounts of Pb-containing NH_4 particles, on the other hand, do not vary significantly except for flight 4, where none are detected (Figure 5). Possible counterions for ammonium are sulfate, nitrate, and chloride. As concluded from the analysis of standard compounds, positive-mode spectra do not provide satisfactory information about the counterion's identity. However, most negative-mode spectra are dominated by the HSO_4^- ion, so SO_4^{2-} seems to be a plausible candidate. This conclusion agrees with the findings of Otten et al. (*8*). The NH_4^+ particles sampled under marine conditions (flights 1 and 2) also appear to contain Na_2SO_4 and, less frequently, NaCl. These probably are internal mixtures of $(NH4)_2SO_4$ with highly transformed sea salt.

Metals detected in these samples are Ba, V, Pb, Cr, Zn, Fe, Ti, Ge, Cd, Sr, Ni, Mn, and Cu. The last six are not included in the discussion. As stated above, Ni, Mn, and Cu suffer too much from spectral interferences to be accurately identified, whereas Ge, Sr, and Cd were detected too sporadically to obtain some conclusive information about them. Table II shows that the incidence with which a metal is detected does not always correspond to its actual concentration in the aerosol, even not when its first ionization potential, which is loosely indicative for the sensitivity, is taken into account. This points to different distributions over particles: e.g., an element might be contained in a huge amount of particles but in a concentration below the detection limit. Finlaysson-Pitts and Pitts (*23*) designate various potential sources of the trace

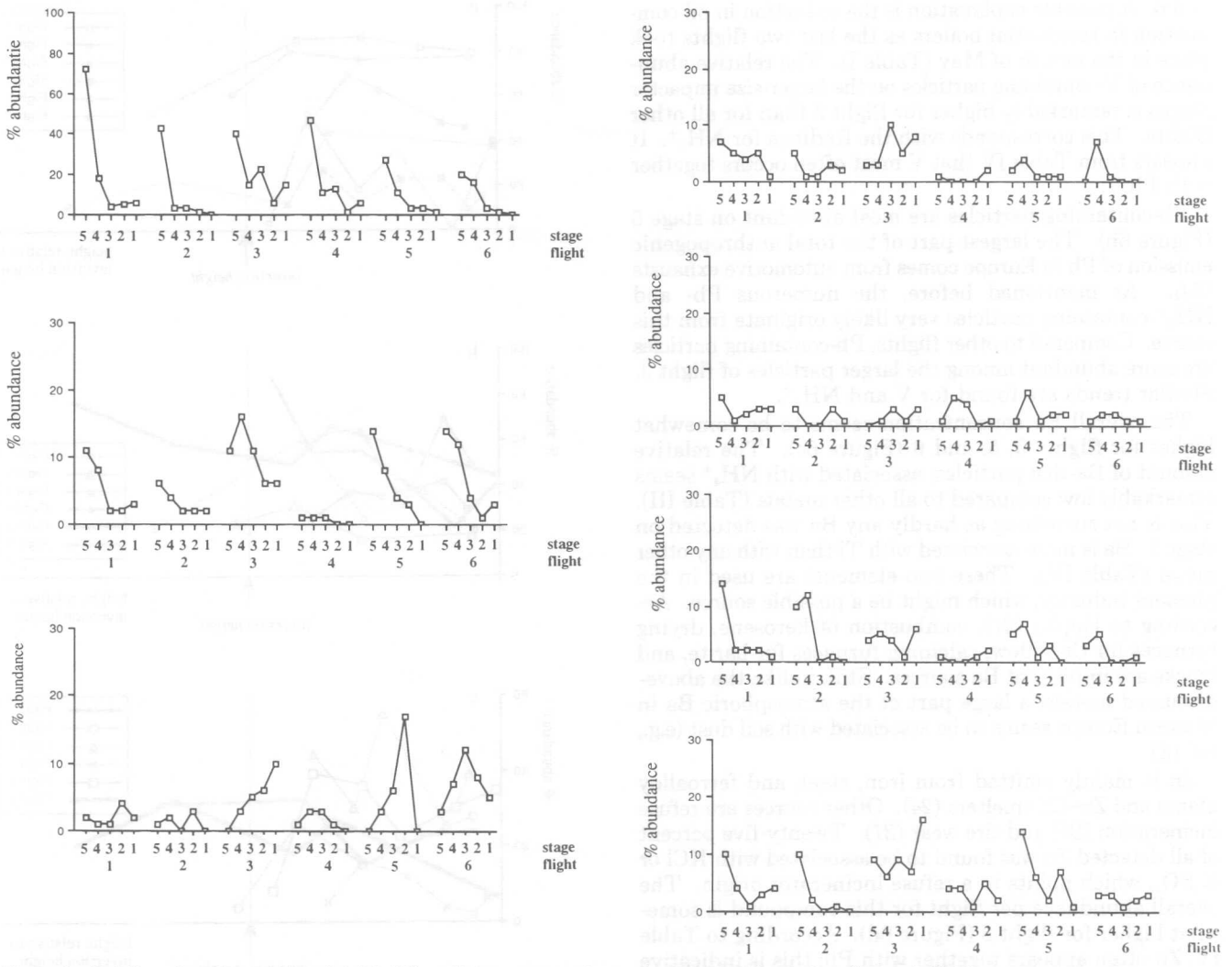

Figure 6. Relative abundances of metal-rich (M) particles, averaged per stage over all impactors for each flight.

Table II. Some Information about Detected Metals

metal	concn in North Sea aerosol, ng·m^{-3} [a]	first ionization potential, eV	detection incidence relative to V
Ba	8	5.21	0.3
V	10	6.74	1.0
Pb	53	7.42	0.4
Cr	3	6.77	0.3
Zn	57	9.89	0.3
Fe	369	7.87	0.4
Ti	27	6.82	0.2

[a] Data from the Kiel Bight (*18*).

Table III. Associations between Metal-Rich Particles, Aluminosilicates, and Ammonium

metal	% metal-rich particles, associated with aluminosilicates	ammonium
V	60	67
Pb	43	60
Ba	65	14
Cr	75	56
Zn	79	41
Fe	65	55
Ti	67	32

Table IV. Mutual Associations between Metals (%) (Not Included in Aluminosilicates)

assocd with	metal V	Pb	Ba	Cr	Zn	Fe	Ti
V		13	2.9	4.9	12	6.5	14
Pb	8.6		2.9	7.3	21	7.6	0
Ba	0.9	1.4		0	3.1	2.6	17
Cr	0.9	2.1	0		10	1.3	3.6
Zn	1.8	4.9	1.5	7.3		1.3	7.1
Fe	2.3	3.5	2.9	2.4	3.1		10
Ti	1.8	0	5.9	2.4	6.3	3.9	

elements found in ambient particulate matter: the combustion of coal and oil, wood burning, waste incineration, metal mining and production, dusts, sea salt, forest fires, volcanic emissions, and emissions from vegetation. Metals detected in this case with LAMMA often occur associated with other compounds, especially with ammonium, with aluminosilicates (Table III), and with other metals (Table IV). For the latter table, metal-rich particles that also exhibit aluminosilicate peaks were not considered in order to obtain an impression about anthropogenic particles (i.e., to rule out soil dust), but in this way, fly ash particles are not considered. As noticed repeatedly above, distinguishing "pure" particles from internal mixtures is not straightforward. In the size profiles of Figure 6, a particle is considered metal-rich when the metal in question appears in the spectrum.

V profiles (Figure 6a) largely correspond to the NH_4^+ profiles of Figure 4. As already mentioned above, V originates from fossil fuel combustion processes. The overall V abundance per flight is somewhat smaller for flights 5

and 6. A possible explanation is the reduction in oil combustion in residential boilers as the last two flights took place in the month of May (Table I). The relative abundance of V-containing particles on the larger-size impactor stages is remarkably higher for flight 3 than for all other flights. This corresponds with the findings for NH_4^+. It appears from Table IV that V most often occurs together with Pb.

Pb-containing particles are most abundant on stage 5 (Figure 6b). The largest part of the total anthropogenic emission of Pb in Europe comes from automotive exhausts (*24*). As mentioned before, the numerous Pb- and NH_4^+-containing particles very likely originate from this source. Compared to other flights, Pb-containing particles are more abundant among the larger particles of flight 3. Similar trends are found for V and NH_4^+.

The overall Ba concentration seems to be somewhat higher for flights 3, 5, and 6 (Figure 6c). The relative amount of Ba-rich particles, associated with NH_4^+ seems remarkably low compared to all other metals (Table III). This is not surprising as hardly any Ba was detected on stage 5. Ba is more associated with Ti than with any other metal (Table IV). These two elements are used in the pigment industry, which might be a possible source. According to Hopke (*21*), combustion of kerosene, drying furnaces for Cr yellow, calcining furnaces for barite, and trucks are important Ba sources. Still, unlike the above-discussed metals, a large part of the atmospheric Ba in Western Europe seems to be associated with soil dust (e.g., ref 18).

Zn is mainly emitted from iron, steel, and ferroalloy plants and Zn–Cd smelters (*24*). Other sources are refuse incineration (*25*) and tire wear (*21*). Twenty-five percent of all detected Zn was found to be associated with KCl or K_2SO_4, which points to a refuse incinerator origin. The overall abundance per flight for this compound is somewhat higher for flight 3 (Figure 6d). According to Table IV, Zn often appears together with Pb; this is indicative of a smelter or alloy-manufacturing origin.

The main source for Ti release in the atmosphere is soil dispersion. Other possibilities are paint spray, agricultural burning, and asphalt production (*21*). Of all metals considered, Ti is mostly associated with Ba.

Cr can be regarded as an indicator of emissions from the iron and steel industry (*24*). This element seems to have a tendency to be concentrated on stages 5 and/or 4 (Figure 6f).

The main Fe sources are soil dust and ferrous metal manufacturing. Fe particles are significantly more abundant for flight 3. They predominantly appear among the smallest particles for flights 1, 2, and 5 (Figure 6g).

Bulk metal analysis (*26*) revealed that absolute Cd, Pb, and Zn concentrations were the highest for flight 3, where the wind direction during sampling was south (Table I). LAMMA for this flight shows increased relative abundances for NH_4^+, V, Pb, Zn, and Fe.

Considering the relative abundances of all investigated compounds as a function of sampling height, no distinct trends could be inferred. As an illustration, panels a–c of Figure 7 shows relative abundances of NaCl, aluminosilicate, and ammonium-rich particles. For each flight, altitudes were referred to the corresponding inversion height (Table I) in order to clarify the representation. Only relative sea salt particle abundances seem to decrease above the inversion layer, which acts as a "lid" on an air mass. Bulk analysis results, on the other hand, show a decrease in *absolute* concentration that rises to a factor of 10 for the metals Cd, Cu, Zn, and Pb.

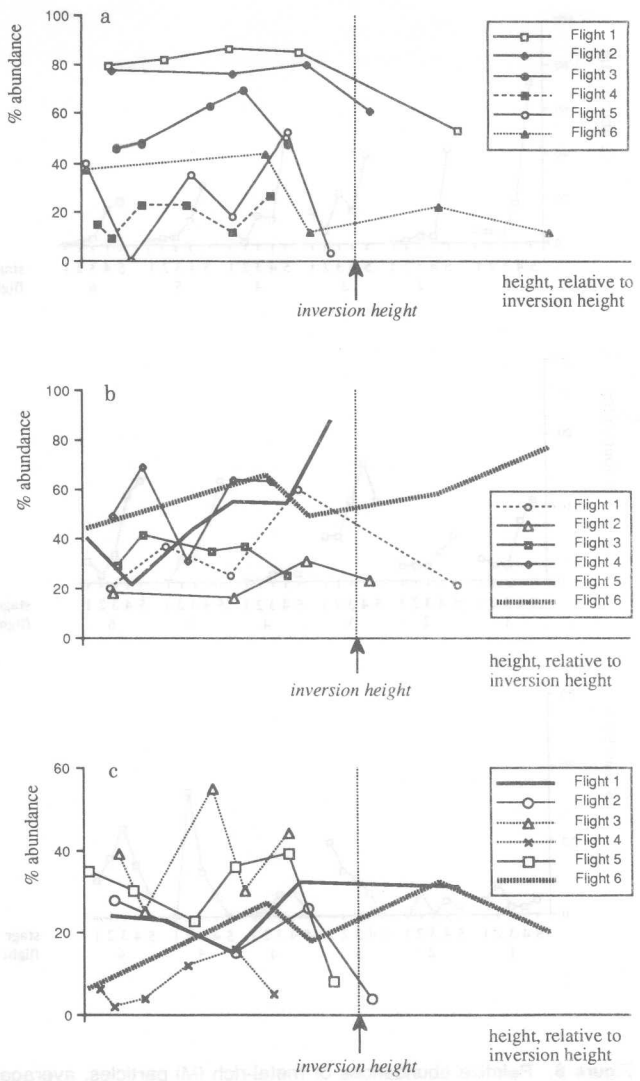

Figure 7. Relative abundances of (a) sea salt particles, (b) aluminosilicates, and (c) ammonium-containing particles as a function of sampling height (altitudes are referred to the corresponding inversion height).

Conclusion

All the individual particle types that have earlier been defined by analyzing North Sea aerosol particles with EPXMA, are detected with LAMMA. However, the particles appear very often as internal mixtures: the image of this aerosol, obtained with LAMMA, is much more complicated.

Examining relative abundances of several compounds of environmental interest as a function of particle size and wind direction during sampling allows some clear trends to be inferred. Ammonium, for example, is mainly present among the smallest particles; sea salt exhibits typical hatlike size profiles and predominates when the sampled air masses have a marine origin. Aluminosilicates and KCl particles prevail for continental air masses.

Better than bulk analysis techniques, LAMMA (and single-particle analysis techniques in general) can provide valuable information about particle origin. If not always conclusive, it does narrow the set of possible sources most of the time: e.g., in the case of the KCl particles, where some alleged sources could be definitely ruled out.

Apart from a decrease in relative sea salt particle concentration above the inversion layer, no definite trends in relative particle type abundances could be deduced as a function of sampling height. This is not surprising as most

sampling was performed beneath the inversion layer.

Registry No. Ba, 7440-39-3; V, 7440-62-2; Pb, 7439-92-1; Cu, 7440-50-8; Zn, 7440-66-6; Fe, 7439-89-6; Ti, 7440-32-6.

Literature Cited

(1) Rojas, C.; Van Grieken, R. *Atmos. Environ.*, in press.
(2) Wouters, L.; Michaud, D.; Van Grieken, R. *Mikrochim. Acta*, submitted.
(3) Verbueken, A.; Bruynseels, F.; Van Grieken, R. In *Inorganic Mass Spectrometry*, 1st ed.; Adams, F., Gijbels, R., Van Grieken, R., Eds.; John Wiley & Sons: New York, 1988; pp 173–256.
(4) Van Espen, P.; Van Vaeck, L.; Adams, F. *Proceedings of the 3rd International LMMS Workshop*; University of Antwerp(UIA): Antwerp, Belgium 1986; pp 195–198.
(5) Pena, J.; Norman, J.; Thomson, D. *J. Air Pollut. Control Assoc.* **1977**, *27*, 337–340.
(6) Xhoffer, C.; Bernard, P.; Van Grieken, R., Van der Auwera, L. *Environ. Sci. Technol.* **1991**, *25*, 1470–1478.
(7) Andreae, M.; Charlson, R.; Bruynseels, F.; Storms, H.; Van Grieken, R.; Maenhout, W. *Science* **1986**, *232*, 1620–1623.
(8) Otten, P.; Bruynseels, F.; Van Grieken, R. *Anal. Chim. Acta* **1987**, *195*, 117–124.
(9) Wouters, L.; Artaxo, P.; Van Grieken, R. *Int. J. Environ. Anal. Chem.* **1990**, *38*, 427–438.
(10) Blanchard, D. In *Air–Sea Exchange of Gases and Particles*, 1st ed.; Liss, P., Slinn, G., Eds.; D. Reidel Publishing Company: Dordrecht, 1983.
(11) Mallant, R.; Kos, G.; Van Wester, A. *Proceedings of the 2nd International Aerosol Conference*; Sept 1986, Berlin; pp 49–52.
(12) Savoie, D. L.; Prospero, J. M. *J. Geophys. Res. Lett.* **1982**, *9*, 1207–1211.
(13) Chessselet, R.; Morelli, J.; Buat-Mênard, P. *J. Geophys. Res.* **1972**, *77*, 5116–5131.
(14) Hoffman, E.; Hoffman, G.; Duce, R. *J. Geophys. Res.* **1980**, *85*, 5499–5502.
(15) Andreae, M. *Science* **1983**, *220*, 1148–1150.
(16) Mamane, Y. *Atmos. Environ.* **1990**, *24B*, 127–137.
(17) Crozat, G. *Tellus* **1979**, *31*, 52–57.
(18) Schneider, B. *Atmos. Environ.* **1987**, *6*, 1275–1283.
(19) Xhoffer, C. Masters Thesis, University of Antwerp, 1988.
(20) Suzuki, T.; Tsunagai, S. *J. Atmos. Chem.* **1988**, *6*, 363–374.
(21) Hopke, P. In *Receptor Modeling in Environmental Chemistry*, 1st ed.; Hopke, P., Ed.; J. Wiley & Sons: New York, 1985.
(22) Biggins, P.; Harrison, B. *Environ. Sci. Technol.* **1980**, *14*, 336–339.
(23) Finlaysson-Pitts, B.; Pitts, J. In *Atmospheric Chemistry: Fundamentals and Experimental Techniques*, 1st ed.; Finlaysson-Pitts, B., Pitts, J., Eds.; J. Wiley & Sons: New York, 1986.
(24) Pacyna, J. *Atmos. Environ.* **1984**, *18*, 41–50.
(25) Mamane, Y. *Atmos. Environ.* **1988**, *22*, 2411–2418.
(26) Injuk, J.; Otten, P.; Laane, R., Maenhaut, W., Van Grieken, R. *Atmos. Environ.*, submitted.

*Received for review November 26, 1991. Accepted December 9, 1991. This work was partially supported by the Dutch Rijkswaterstaat, Den Haag, The Netherlands, through Project NOVIME*2 Tasks No. DGW-920 and DGW-217 and by the Belgian Ministry of Science Policy through Project EUR/7/90. D.M. acknowledges a leave grant from the Ministry of Education, Québec, Canada.*